Inorg. Chem. **2007**, *46*, 10827–10839

Vanadium Complexes Possessing $N_2O_2S_2$-Based Ligands: Highly Active Procatalysts for the Homopolymerization of Ethylene and Copolymerization of Ethylene/1-hexene

Damien M. Homden, Carl Redshaw,* and David L. Hughes

School of Chemical Sciences and Pharmacy, University of East Anglia, Earlham Road, Norwich, Norfolk NR4 7TJ, UK

Received July 23, 2007

The family of ligands containing an $N_2O_2S_2$ core, namely, 1,2-di(3-Me-5-*t*-Bu-salicylaldimino-*o*-phenylthio)ethane (**H_2L^1**), 1,3-di(3-Me-5-*t*-Bu-salicylaldimino-*o*-phenylthio)propane (**H_2L^2**), 1,4-di(3-Me-5-*t*-Bu-salicylaldimino-*o*-phenylthio)-butane (**H_2L^3**), and 1,2-di(3-Me-5-*t*-Bu-salicylaldamino-*o*-phenylthio)ethane (**H_2L^4**), have been prepared and complexed with a variety of vanadium chlorides and alkoxides to afford complexes of the form [V(X)L^1] (X = O (**1**), N*p*-tol (**2**), Cl (**3**)), [V(O)($L^{2,3}$)] (L^2 (**4**), L^3 (**5**)), and [V(L^4)] (**6**). Crystal structure determinations of **H_2L^1** and **H_2L^4** show the molecule to be centrosymmetric about the bridging ethane moiety, with structural determination of **1** and **3** revealing isostructural monomeric complexes in which the ligand chelates in such a way as to afford pseudo-octahedral coordination at the vanadium center. Prolonged reaction of **H_2L^1** with [V(N*p*-tol)$(OEt)_3$] led, via oxidative cleavage of the C–S bond, to the bimetallic complex [V_2L^1(3-Me,5-*t*-Bu-salicylaldimino-*o*-phenylthiolate)$_2$] **[VL′]** (**7**), as characterized by single-crystal X-ray crystallography. **7** was also isolated from the reaction of **H_2L^4** and [VO(O*n*-Pr)$_3$]. The ability of **1**–**7** to catalyze the homopolymerization of ethylene and the copolymerization of ethylene/1-hexene in the presence of dimethylaluminum chloride (DMAC) has been assessed: screening reveals that for ethylene homopolymerization **1**–**7** are all highly active (>1000 g/mmol·h·bar), with the highest activity (ca. 11 000 g/mmol·h·bar) observed using catalyst **3**; the use of trimethyl aluminum (TMA) or methylaluminoxane (MAO) as the cocatalyst led only to poorly active systems producing negligible polymer. Analysis of the polyethylene produced showed high molecular weight linear polymers with narrow polydispersities. For ethylene/1-hexene copolymerization, activities as high as 1 190 g/mmol·h·bar were achieved (**4**); analysis of the copolymer indicated an incorporation of 1-hexene in the range of 5–13%.

1. Introduction

Group IV metallocenes, half-sandwich, and constrained geometry catalysts have generated significant interest in the field of Ziegler−Natta olefin polymerization, and as a result numerous patents have been filed on such systems.[1,2] Motivated by the desire from industry to gain increased control over polymer properties and to steer away from well-established licensed technology, focus into nonmetallocene-based catalytic systems has steadily risen since the mid 1990s.[3,4] In contrast to the high activities observed for the group IV metal systems, the successful use of group V metals has been somewhat limited,[5,6] this despite the commercial use of the [V$(acac)_3$] system in the production of ethylene-propylene-diene elastomers.[7] The beneficial properties of vanadium-based catalysis were recognized at an early stage by Natta et al.; [V$(acac)_3$] or [VCl_4] in combination with a variety of different organoaluminum cocatalysts led to the preparation of highly stereospecific syndiotactic polypropylene polymers.[8] More recently, vanadium catalysts have been

* To whom correspondence should be addressed. E-mail: carl.redshaw@uea.ac.uk, Tel +44 (0) 1603 593137.

(1) McKnight, A. L.; Waymouth, R. M. *Chem. Rev.* **1998**, *98*, 2587.
(2) Brintzinger, H. H. *Angew. Chem., Int. Ed. Engl.* **1995**, *34*, 1368.
(3) Gibson, V. C.; Britovsek, G. J. P.; Wass, D. F. *Angew. Chem., Int. Ed.* **1999**, *38*, 428.
(4) Gibson, V. C.; Spitzmesser, S. K. *Chem. Rev.* **2003**, *103*, 283.
(5) van Koten, G.; Hagen, H.; Boersma, J. *Chem. Soc. Rev.* **2002**, *31*, 357.
(6) Gambarotta, S. *Coord. Chem. Rev.* **2003**, *237*, 229.
(7) Kaminsky, W.; Arndt, M. *Applied Homogeneous Catalysis with Organometallic Compounds*; Cornils, B., Hermann, W. A., Eds.; VCH Publishers: Weinheim, Germany, 1996; Vol. 1, pp. 220.
(8) Natta, G.; Zambelli, A.; Pasquon, I. *J. Am. Chem. Soc.* **1962**, *84*, 1488.

10.1021/ic701461b CCC: $37.00
Published on Web 11/09/2007

Scheme 1. Recent Sulfur-Bridged Diphenolate Early Transition Metal Complexes of (a) Group IV and (b) Group V

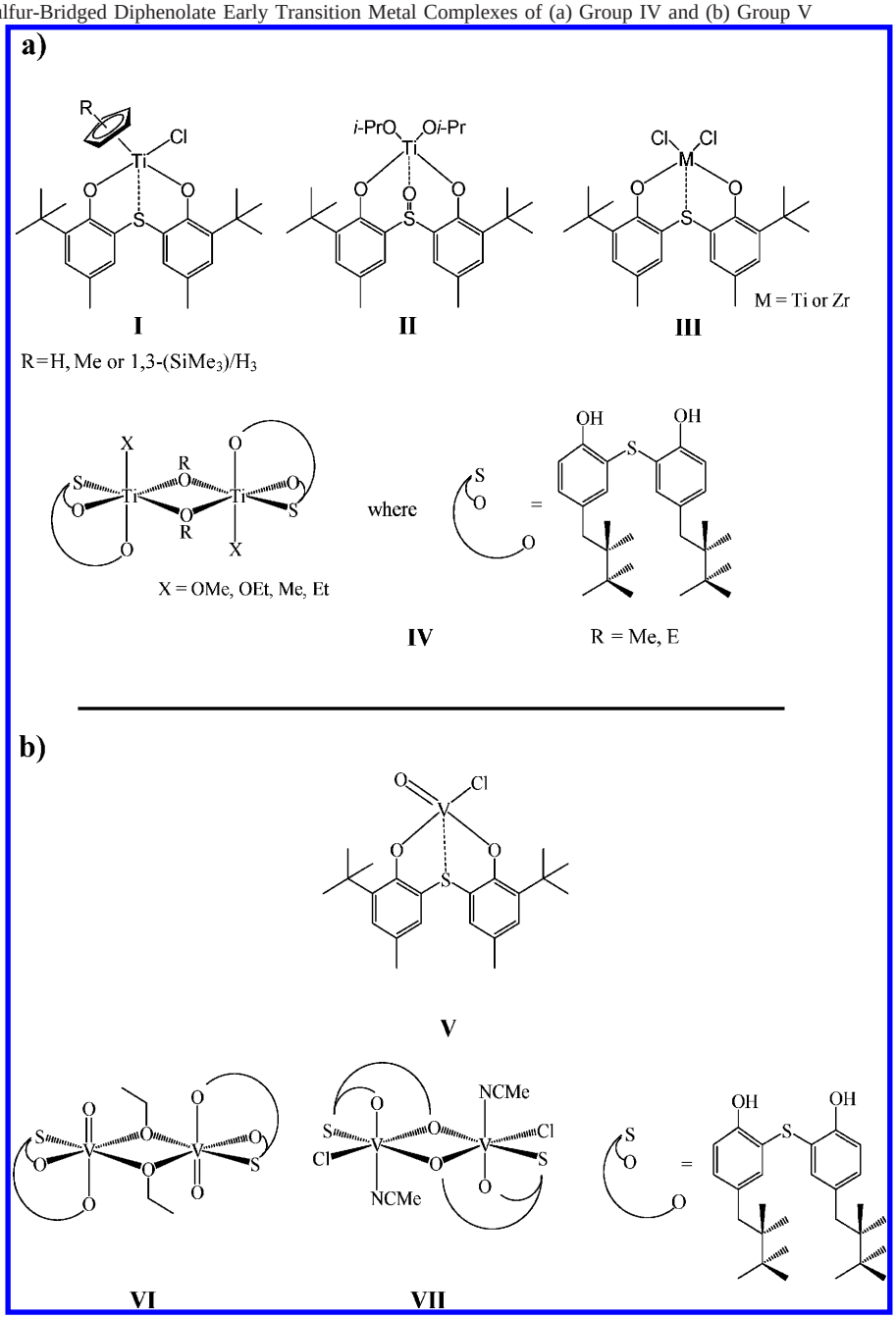

utilized in both homo- and hetero-geneous systems and are found to be capable of producing polymers with ultrahigh molecular weights and narrow polydispersities.[9−13] Redshaw et al., Gibson et al., and Nomura et al. have demonstrated highly active group V catalysts[14−24] utilizing bi- or tridentate ligands, whereas a $MgCl_2$-supported vanadium phenoxy-imine system has been reported by Fujita and Matsui.[25] The ease of reduction of the metal center to the lower inactive state (divalent for vanadium) constitutes one of the intrinsic problems associated with group V catalysts, though the use of reactivating agents such as ethyltrichloroacetate (ETA) or chlorinated hydrocarbons is a useful method for maintaining the higher (active) oxidation states of vanadium systems.[6,14,16,27] The situation is compounded by the highly sensitive nature of cationic group V metal alkyls.[15,26]

Previous aryloxide-based chemistry carried out upon group IV metals (titanium and zirconium) has shown enhanced catalytic activity for diphenolate ligands bearing bridging sulfur atoms, for example, **I**−**IV** (part a of Scheme 1).[28−30] In particular, Schaverien et al.[29] found that the additional

(9) Casagrande, A. C. A.; dos Anjos, P. S.; Gamba, D.; Casagrande, O. L.; dos Santos, J. H. Z. *J. Mol. Catal. A: Chem.* **2006**, *255*, 19.
(10) Huang, R. B.; Kukalyekar, N.; Koning, C. E.; Chadwick, J. C. *J. Mol. Catal. A: Chem.* **2006**, *260*, 135.
(11) Casagrande, A. C. A.; Tavares, T. T. D.; Kuhn, M. C. A.; Casagrande, O. L.; dos Santos, J. H. Z.; Teranishi, T. *J. Mol. Catal. A: Chem.* **2004**, *212*, 267.
(12) Wang, W.; Yamada, J.; Fujiki, M.; Nomura, K. *Catal. Commun.* **2003**, *4*, 159.
(13) Kotov, V. V.; Avtomonov, E. V.; Sundermeyer, J.; Aitola, E.; Repo, T.; Lemenovskii, D. A. *J. Organomet. Chem.* **2001**, *640*, 21.
(14) Gibson, V. C.; Tomov, A. K.; Zaher, D.; Elsegood, M. R. J.; Dale, S. H. *Chem. Commun.* **2004**, 1956.

Scheme 2. Synthesis of Ligands $\mathbf{H_2L^{1-4}}$ [a]

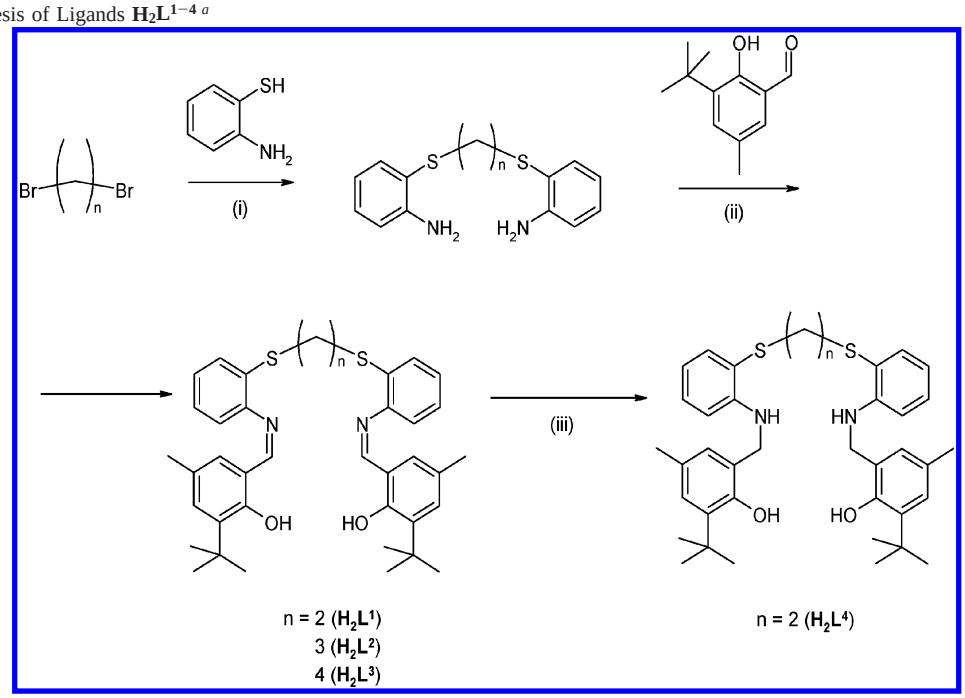

[a] (i) Dry ethanol and Na. (ii) EtOH/H^+(cat), reflux 12 h. (iii) THF, $LiAlH_4$, room temperature, with stirring.

flexibility and potential π donation from the inclusion of a sulfur atom in [Ti(tbmp)Cl_2] (**III**, M = Ti) (where tbmp = 2,2′-thiobis(6-*t*-Bu-4-methylphenolato)) led to a 10-fold increase in catalytic activity for ethylene polymerization. The procatalysts [Ti(tbmp)(NR_2)] (R = Me, Et) have been evaluated for the polymerization of ϵ-caprolactone;[31] the additional sulfur interaction led to a more efficient initiation of the polymerization and a lower spread of molecular weights of the resulting polymer. Furthermore, the complexes [Ti(tmbp)X_2] (X = Cl, O*i*-Pr) exhibit high activities (20 000−43 000 g/mmol·h·bar) for the copolymerization of ethylene/styrene (up to 100 times greater); the methylene analogue (replacing the bridging sulfur atom) produces only a mixture of homopolyethylene and homopolystyrene.[28] In the case of vanadium, Miyatake et al.[32] showed that the complexes [V(O)(tbmp)X] (X = Cl, OC_4H_9) (part b of Scheme 1, **V**) upon activation with methylaluminoxane produced activities over 100 times greater for propylene polymerization than their unsupported (e.g., $VOCl_3$) vanadium counterparts; the resulting polypropylene was isotactically enriched (mm % > 35%), with a significantly narrower polydispersity. Although no catalytic enhancement was observed in the $MgCl_2$-supported procatalysts [$V_2(\mu$-OEt)$_2$(O)$_2$(tbop-κ^3O,S,O)$_2$] and [$V_2(\mu$-tbop-κ^3O,S,O)$_2$$Cl_2$($CH_3CN$)$_2$] (where tbop = 2,2′-thiobis{4-(1,1,3,3-tetramethyl-butyl)phenol} (part b of Scheme 1, **VI** and **VII**),[33] it was found that the stability of the active species during the polymerization reaction was increased and displayed only a slight decrease in activity of the catalyst over a 3 h period.

To date, examples of complexes where the ancillary ligand incorporates sulfur, nitrogen, and oxygen donors are primarily focused on biological applications as bifunctional chelating agents for radioimaging with ^{99m}Tc[34,35] or mimics for iron(II/III) in enzymes within the body,[36,37] whereas sulfur,

(15) Nomura, K.; Wang, W. *Macromolecules* **2005**, *38*, 5905.
(16) Redshaw, C.; Warford, L.; Dale, S. H.; Elsegood, M. R. J. *Chem. Commun.* **2004**, 1954.
(17) Redshaw, C.; Rowan, M. A.; Homden, D. M.; Dale, S. H.; Elsegood, M. R. J.; Matsui, S.; Matsuura, S. *Chem. Commun.* **2006**, 3329.
(18) Redshaw, C.; Homden, D. M.; Rowan, M. A.; Elsegood, M. R. J. *Inorg. Chim. Acta* **2005**, *358*, 4067.
(19) Mountford, P.; Bigmore, H. R.; Zuideveld, M. A.; Kowalczyk, R. M.; Cowley, A. R.; Kranenburg, M.; McInnes, E. J. L. *Inorg. Chem.* **2006**, *45*, 6411.
(20) Jaffart, J.; Nayral, C.; Choukroun, R.; Mathieu, R.; Etienne, M. *Eur. J. Inorg. Chem.* **1998**, 425.
(21) Mashima, K.; Nakayama, Y.; Ikushima, N.; Kaidzu, M.; Nakamura, A. *J. Organomet. Chem.* **1998**, *566*, 111.
(22) Green, M. L. H.; Chen, C. T.; Doerrer, L. H.; Williams, V. C. *J. Chem. Soc., Dalton Trans.* **2000**, 967.
(23) Gibson, V. C.; Coles, M. P.; Dalby, C. I.; Little, I. R.; Marshall, E. L.; da Costa, M. H. R.; Mastroianni, S. *J. Organomet. Chem.* **1999**, *591*, 78.
(24) Nakamura, A.; Mashima, K.; Fujikawa, S.; Tanaka, Y.; Urata, H.; Oshiki, T.; Tanaka, E. *Organometallics* **1995**, *14*, 2633.
(25) Fujita, T.; Matsui, S. *Catal. Today* **2001**, *66*, 63.
(26) Etienne, M.; Pritchard, H. M.; Vendier, L.; McGrady, G. S. *Organometallics* **2004**, *23*, 1203.
(27) Desmangles, N.; Gambarotta, S.; Bensimon, C.; Davis, S.; Zahalka, H. *J. Organomet. Chem.* **1998**, *562*, 53.
(28) Mulhaupt, R.; Sernetz, F. G.; Fokken, S.; Okuda, J. *Macromolecules* **1997**, *30*, 1562.
(29) Schaverien, C. J.; Vanderlinden, A.; Meijboom, N.; Ganter, C.; Orpen, A. G. *J. Am. Chem. Soc.* **1995**, *117*, 3008.
(30) Sobota, P.; Janas, Z.; Jerzykiewicz, L. B.; Przybylak, K.; Szczegot, K. *Eur. J. Inorg. Chem.* **2004**, 1639.
(31) Takashima, Y.; Nakayama, Y.; Hirao, T.; Yasuda, H.; Harada, A. *J. Organomet. Chem.* **2004**, *689*, 612.
(32) Takaoki, K.; Miyatake, T. *Macromol. Symp.* **2000**, *157*, 251.
(33) Janas, Z.; Wisniewska, D.; Jerzykiewicz, L. B.; Sobota, P.; Drabent, K.; Szczegot, K. *Dalton Trans.*, **2007**, 2065.
(34) Dhara, P. K.; Das, B.; Lo, J. M.; Chattopadhyay, P. *Appl. Radiat. Isot.* **2005**, *62*, 729.
(35) Chhikara, B. S.; Kumar, N.; Tandon, V.; Mishra, A. K. *Bioorg. Med. Chem.* **2005**, *13*, 4713.
(36) Sellmann, D.; Blum, D. C. F.; Heinemann, F. W.; Sutter, J. *Eur. J. Inorg. Chem.* **2003**, 418.
(37) Singh, A. K.; Mukherjee, R. *Inorg. Chem.* **2005**, *44*, 5813.

Table 1. Crystallographic Data and Results of X-ray Analysis

compound	H_2L^1	H_2L^4	**1**	**3**	**7**
formula	$C_{38}H_{44}N_2O_2S_2$	$C_{38}H_{48}N_2O_2S_2$	$C_{38}H_{42}N_2O_3S_2V.MeCN$	$C_{38}H_{42}ClN_2O_2S_2V.MeCN$	$C_{74}H_{80}N_4O_4S_4V_2.2Et_2O$
fw	624.9	628.9	730.8	750.3	1467.8
cryst syst	monoclinic	monoclinic	triclinic	triclinic	triclinic
space group	$P2_1/a$	$C2/c$	$P\bar{1}$	$P\bar{1}$	$P\bar{1}$
unit cell dimensions					
a (Å)	9.3754(7)	16.5584(15)	9.6480(1)	9.6892(7)	11.567(3)
b (Å)	17.3669(11)	7.7388(6)	11.9119(2)	11.7442(10)	12.515(3)
c (Å)	11.1490(7)	27.125(3)	16.9911(3)	17.1594(8)	14.789(4)
α (deg)	90	90	83.830(1)	84.560(6)	73.40(2)
β (deg)	116.819(7)	100.499(8)	85.870(1)	84.449(6)	80.22(2)
γ (deg)	90	90	73.428(1)	76.692(7)	65.98(2)
V (Å^3)	1620.04(19)	3417.6(6)	1859.01(5)	1885.9(2)	1870.4(8)
Z	2	4	2	2	1
T (K)	140(1)	140(1)	120(1)	140(1)	140(1)
D_{calcd} (g cm^{-3})	1.281	1.222	1.306	1.321	1.303
absorption coefficient (mm^{-1})	0.202	0.191	0.420	0.483	0.417
cryst size (mm^3)	0.6 × 0.24 × 0.06	0.64 × 0.40 × 0.13	0.12 × 0.06 × 0.04	0.73 × 0.24 × 0.10	0.48 × 0.22 × 0.14
2θ max (deg)	55	50	55	60	40
reflns measured	21 255	18 200	42 231	28 521	11 010
unique reflns	3699	2990	8520	10 633	3434
R_{int}	0.047	0.056	0.055	0.072	0.100
reflns with $F^2 > 2\sigma(F^2)$	3382	2454	6828	6842	2648
transmission factors		0.986−1.015	0.816−1.00	0.945−1.064	0.972−1.031
number of params	204	203	445	445	444
R_1 [$F^2 > 2\sigma(F^2)$]	0.049	0.055	0.044	0.044	0.100
wR_2, R_1 (all data)	0.125, 0.056	0.105, 0.077	0.107, 0.061	0.093, 0.089	0.190, 0.132
largest difference peak and hole (e Å^{-3})	0.35 and −0.27	0.46 and −0.35	0.39 and −0.52	0.63 and −0.51	0.42 and −0.36

nitrogen, and oxygen donor ligands in combination with vanadium are limited to the use of thiosemicarbazones.[38−40]

It is noteworthy that a number of vanadium-based catalytic systems for use in α-olefin polymerization have appeared in the patent literature. In particular, systems of the type $V_2X_3(ED)_n$ where X = halogen and ED = electron-donating groups such as ethers, phosphine, ketones, isocyanides, or esters in conjunction with organoaluminum cocatalysts and a halocarbon promoter[41,42] have been reported, as well as systems supported on silica.[43]

Taking into account the high activity afforded by phenoxyimine ligands and the beneficial effects imparted by donor sulfur atoms in the aforementioned diphenolate-based systems, we decided to examine a family of ligands incorporating both of these potentially desirable features and to screen for possible beneficial effects in vanadium-catalyzed α-olefin polymerization. Herein, the synthesis and characterization of four new ligands **H_2L^1**−**H_2L^4** (Scheme 2, section 3.1), the new vanadium complexes [V(X)L^1] (X = O (**1**), N*p*-tol (**2**), Cl (**3**)), [V(O)($L^{2,3}$)] (L^2 (**4**), L^3 (**5**)) and [V(L^4)] (**6**), together with the bimetallic complex [V_2L^1-(3-Me,5-*t*-Bu-salicylaldimino-*o*-phenylthiolate)$_2$] (**7**) (Scheme 4, section 3.3) are reported. In addition, **1**−**7** have been screened for ethylene homopolymerization and ethylene/1-hexene copolymerization in the presence of the organoaluminum cocatalyst dimethylaluminum chloride (DMAC) and the reactivating substance ETA.

2. Experimental Section

All of the manipulations were carried out under an atmosphere of nitrogen using standard Schlenk line and cannula techniques or a conventional N_2-filled glovebox. Solvents were refluxed over the appropriate drying agents and distilled and degassed prior to use. Elemental analyses were performed at London Metropolitan University. NMR spectra were recorded on a Varian VXR 400 S spectrometer at 400 MHz, a Gemini at 300 MHz, or a Bruker DPX300 spectrometer at 300 MHz (^{1}H) and 75.5 MHz (^{13}C) at 298 K; chemical shifts are referenced to the residual protio impurity of the deuterated solvent. EPR spectroscopy was performed on an X-band ER200-D spectrometer (Bruker Spectrospin) interfaced to an ESP1600 computer and fitted with a liquid-helium flow cryostat (ESR-900; Oxford Instruments), and the spectra were simulated with Simfonia. IR spectra (nujol mulls, KBr windows) were recorded on a PerkinElmer 577 or 457 grating spectrophotometer. DSC analyses of polymer samples were performed on a TA Instruments DSC Q 1000. Magnetic moments were recorded following the Evans' NMR method.[44] 1,2-Bis(2-aminophenylthio)-ethane (**A**), 1,3-bis(2-aminophenylthio)propane (**B**), 1,4-bis(2-aminophenylthio)butane (**C**), and the known procatalysts **8** and **9** were synthesized following the reported procedures;[35,45,46] [VO(O*n*-Pr)$_3$] was purchased from Aldrich and used as received. [V(N*p*-tol)(OEt)$_3$] and [VCl_3·3THF] were synthesized following the reported procedures by van Koten et al.[47] and Kurras.[48] All of the

(38) Sreekanth, A.; Sivakumar, S.; Kurup, M. R. P. *J. Mol. Struct.* **2003**, *655*, 47.
(39) Khuhawar, M. Y.; Arain, G. M. *Talanta* **2006**, *68*, 535.
(40) Maurya, M. R.; Kumar, A.; Abid, M.; Azam, A. *Inorg. Chim. Acta* **2006**, *359*, 2439.
(41) Stakem, F. G. *Eur. Pat. Appl.* **1990**, 9 pp, EP 374595 A1.
(42) Beran, D. L.; Cann, K. J.; Jorgensen, R. J.; Karol, F. J.; Maraschin, N. J.; Marcinkowsky, A. E. *Eur. Pat. Appl.* **1984**, 35 pp. EP 120501 A1.
(43) Wagner, B. E.; Samuels, Sari, B.; Karol, F. J. *Eur. Pat. Appl.* **1992**, 16 pp, EP 464744 A2.
(44) Evans, D. F. *J. Chem. Soc.* **1959**, 2003.
(45) Donaldson, P. B.; Tasker, P. A.; Alcock, N. W. *J. Chem. Soc., Dalton Trans.* **1976**, 2262.
(46) Nakayama, Y.; Bando, H.; Sonobe, Y.; Suzuki, Y.; Fujita, T. *Chem. Lett.* **2003**, *32*, 766.
(47) Lutz, M.; Hagen, H.; Schreurs, A. M. M.; Spek, A. L.; van Koten, G. *Acta Crystallogr.* **1999**, *C55*, 1636.

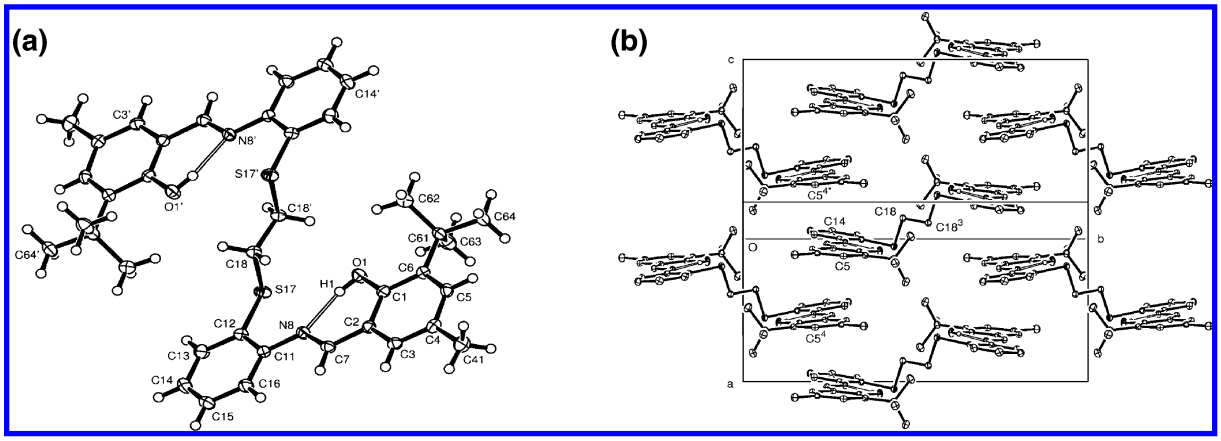

Figure 1. (a) View of a molecule of $\mathbf{H_2L^1}$ showing the atom numbering scheme. Thermal ellipsoids are drawn at the 50% probability level. (b) Packing diagram showing the intercalation of planar phenoxy-imine groups.

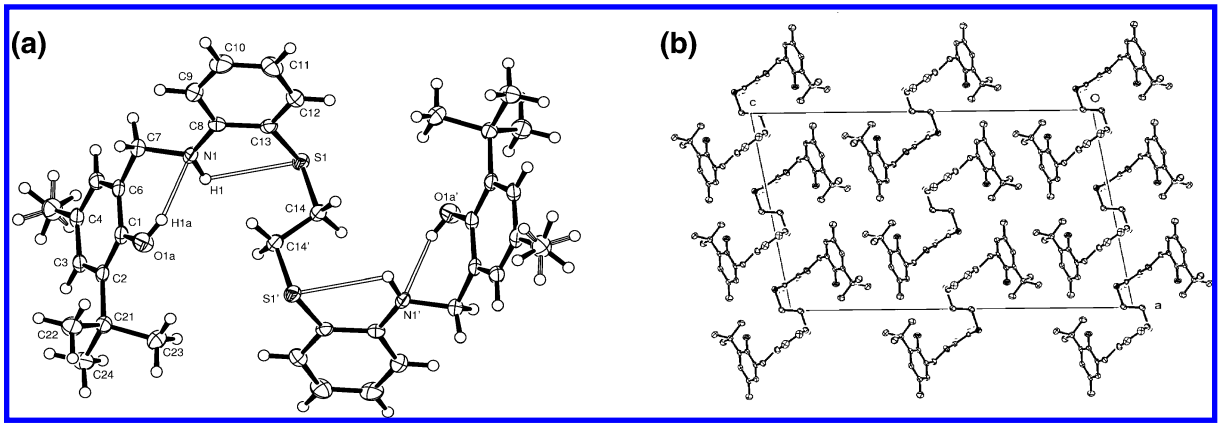

Figure 2. (a) View of a molecule of $\mathbf{H_2L^4}$, showing disorder in the methyl group at C(4). Thermal ellipsoids are drawn at the 50% probability level. (b) Packing diagram looking down the *b* axis.

other chemicals were obtained commercially and used as received unless stated otherwise.

2.1. Synthesis of Ligands. 2.1.1. Preparation of 1,2-Di(4-Me-6-*t*-Bu-salicylaldimino-*o*-phenylthio)ethane ($\mathbf{H_2L^1}$). 1,2-Bis(2-aminophenylthio)ethane (2.20 g, 7.96 mmol) and 3-Me-5-*t*-Bu-salicaldehyde (1.53 g, 7.96 mmol) were brought to reflux in ethanol (25 mL). A drop of formic acid was added to catalyze the reaction, and the reflux maintained for 12 h. Upon cooling, the solvent was removed in vacuo, affording $\mathbf{H_2L^1}$ as an orange solid. Yield 3.63 g (73%). Mp 153−155 °C. Anal. Found: C, 73.0; H, 7.1; N, 4.5. $C_{38}H_{44}N_2O_2S_2$ requires: C, 72.6; H, 7.1; N, 4.4. ^{1}H NMR ($CDCl_3$): δ 8.52 (s, 2H, CH═N), 7.11−7.40 (m, 12H, ArH), 7.02 (s, 2H, OH), 3.15 (s, 3H, Me), 2.31 (s, 4H, CH_2), 1.46 (s, 18H, *t*-Bu). Mass Spec. (ESI): 625 $(M)^+$. IR (cm^{-1}): ν 3580 m, 1615 m, 1588 m, 1574 m, 1559 m, 1463 s, 1377 m, 1322 m, 1267 m, 1231 w, 1203 m, 1153 m, 1126 w, 1060 w, 1040 s, 1021 s, 959 w, 893 w, 854 m, 772 m, 749 m, 718 m, 665 m.

2.1.2. Preparation of 1,3-Di(3-Me-5-*t*-Bu-salicylaldimino-*o*-phenylthio)propane ($\mathbf{H_2L^2}$). As for $\mathbf{H_2L^1}$ but using 1,3-bis(2-aminophenylthio)propane (2.00 g, 6.89 mmol) and 3-Me-5-*t*-Bu-salicaldehyde (2.78 g, 14.46 mmol) to give a yellow oil. This was further purified by extraction into hexane (30 mL) and stored at 0 °C for 1 week to give $\mathbf{H_2L^2}$ as a yellow oil. Yield 3.70 g (84%). Anal. Found: C, 73.4; H, 7.2; N, 4.2. $C_{39}H_{46}N_2O_2S_2$ requires: C, 73.3; H, 7.3; N, 4.4. ^{1}H NMR ($CDCl_3$): δ 8.54 (s, 2H, CH═N), 7.35−7.05 (m, 12H, ArH), 3.08 (t, 4H $^3J_{HH}$ 7.0 Hz, CH_2), 2.31 (s, 6H, Me), 2.06 (quin, 2H $^3J_{HH}$ 7.2 Hz, CH_2), 1.46 (s, 18H, *t*-Bu). Mass Spec. (ESI): 639 $(M)^+$. IR (cm^{-1}): ν 3582 m, 3457 bm, 3370 bm, 3057 m, 2956 s, 2921 s, 2863 m, 2359 m, 2325 m, 2245 m, 1936 w, 1726 w, 1614 s, 1573 s, 1563 s, 1469 s, 1435 s, 1390 m, 1360 m, 1264 s, 1235 m, 1205 m, 1162 m, 1067 m, 1029 m, 980 m, 908 s, 864 m, 801 m, 753 m, 732 m, 666 m, 648 m.

2.1.3. Preparation of 1,4-Di(3-Me-5-*t*-Bu-salicylaldimino-*o*-phenylthio)butane ($\mathbf{H_2L^3}$). As for $\mathbf{H_2L^1}$ but using 1,4-bis(2-aminophenylthio)butane (2.00 g, 6.57 mmol) and 3-Me-5-*t*-Bu-salicaldehyde (2.65 g, 13.79 mmol) to give a yellow oil. This was further purified by extraction into hexane (30 mL) and stored at 0 °C for 1 week to give $\mathbf{H_2L^3}$ as a yellow solid. Yield 1.71 g (40%). Mp 81−84 °C. Anal. Found: C, 73.5; H, 7.6; N, 4.2. $C_{40}H_{48}N_2O_2S_2$ requires: C, 73.6; H, 7.4; N, 4.3. ^{1}H NMR ($CDCl_3$): δ 8.48 (s, 2H, CH═N), 7.39−6.85 (m, 12H, ArH), 2.81 (s, 4H, CH_2), 2.23 (s, 6H, Me), 1.78 (s, 4H, CH_2), 1.47 (s, 18H, *t*-Bu). Mass Spec. (ESI): 653 $(M)^+$. IR (cm^{-1}): ν 3146 bm, 2361 m, 2341 m, 1745 w, 1617 m, 1594 m,1575 m, 1563 m,1322 m, 1263 m, 1236 m, 1205 m, 1162 m, 1067 m, 981 m, 961 w, 927 w, 857 m, 800 s, 770 m, 751 m, 740 m, 721 m, 668 w.

2.1.4. Preparation of 1,2-Di(3-Me-5-*t*-Bu-salicylaldamino-*o*-phenylthio)ethane ($\mathbf{H_2L^4}$). To a solution of $\mathbf{H_2L^1}$ (1.35 g, 2.16 mmol) in THF (50 mL) was added $LiAlH_4$ (0.33 g, 8.64 mmol) in small portions at room temperature. Over 5 min, the solution turns from a dark orange/yellow to a very light yellow. Once the color change had ceased, the solution was stirred for a further 30 min. The solvents were removed in vacuo, and the residue cooled to 0 °C. Chilled water (100 mL) was added slowly, followed by the addition of Et_2O (200 mL). The organic phase was collected,

(48) Kurras, E., *Naturwissenschaften* **1959**, *46*, 171.

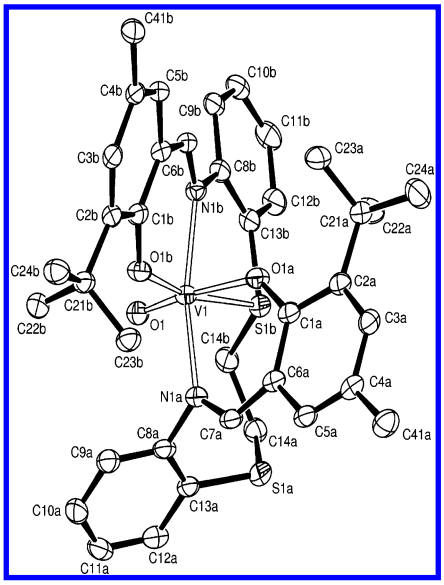

Figure 3. View of a molecule of **1** showing the atom numbering scheme. Thermal ellipsoids are drawn at the 50% probability level.

Table 2. Comparison of Selected Bond Lengths (Angstroms) and Angles (Degrees) in **1** and **3**

1		**3**	
V(1)−O(1)	1.6193(14)	V−Cl	2.3717(6)
V(1)−O(1A)	2.0294(14)	V−O(1B)	1.9096(13)
V(1)−O(1B)	1.9209(14)	V−O(1A)	1.8704(13)
V(1)−N(1A)	2.1037(16)	V−N(8B)	2.1006(16)
V(1)−N(1B)	2.0883(16)	V−N(8A)	2.0788(16)
V(1)−S(1B)	2.5252(6)	V−S(17A)	2.5403(6)
O(1)−V(1)−O(1A)	168.27(7)	Cl−V−O(1B)	171.00(4)
O(1)−V(1)−O(1B)	100.47(7)	Cl−V−O(1A)	91.43(4)
O(1)−V(1)−N(1A)	95.66(7)	Cl−V−N(8B)	95.40(4)
O(1)−V(1)−N(1B)	98.68(7)	Cl−V−N(8A)	92.08(4)
O(1)−V(1)−S(1B)	88.92(5)	Cl−V−S(17A)	88.275(19)
N(1A)−V(1)−N(1B)	164.93(7)	N(8A)−V−N(8B)	172.01(6)
S(1B)−V(1)−O(1A)	79.55(4)	S(17A)−V−O(1B)	82.76(4)
O(1A)−V(1)−O(1B)	91.24(6)	O(1A)−V−O(1B)	97.31(6)
O(1B)−V(1)−S(1B)	167.94(5)	O(1A)−V−S(17A)	171.03(4)

washed with a 10% HCl solution (50 mL) and water (2 × 50 mL), respectively, and dried over $MgSO_4$. Removal of the Et_2O in vacuo and recrystallization of the solid from ethanol gave $\mathbf{H_2L^4}$ as yellow blocks. Yield of crystals, 500 mg (30%). Total yield (1.11 g, 82%). Mp 115 °C. Anal. Found: C, 72.6; H, 7.7; N, 4.5. $C_{38}H_{48}N_2O_2S_2$ requires: C, 72.5; H, 7.6; N, 4.5. ^{1}H NMR ($CDCl_3$): δ 8.06 (s, 2H, OH), 6.60−7.40 (m, 12H, ArH), 5.16 (s, 2H, NH), 4.32, (s, 4H, CH_2N), 2.80, (s, 4H, SCH_2), 1.40, (s, 18H, *t*-Bu). Mass Spec. (ESI): 629 $(M)^+$. IR (cm^{-1}): ν 3156 m, 3107 m, 1580 m, 1300 m, 1269 m, 1231 w, 1215 w, 1192 m, 1153 w, 1075 w, 1029 w, 1005 m, 966 w, 932 w, 897 w, 854 w, 800 w, 745 m, 717 m.

2.2. Synthesis of Complexes. 2.2.1. Preparation of [V(O)L^1] (1). [V(O)(O*n*-Pr)$_3$] (0.40 mL, 1.76 mmol) and $\mathbf{H_2L^1}$ (1.00 g, 1.60 mmol) were refluxed for 12 h in toluene (40 mL). After cooling, the solvent was removed in vacuo, and the residue was extracted into warm acetonitrile (40 mL), affording **1** as deep-red prisms. Yield 786 mg (71%). Mp > 250 °C. Anal. Found: C, 65.7; H, 6.2; N, 5.8. $C_{38}H_{42}N_2O_3S_2V\cdot$MeCN requires: C, 65.3; H, 6.2; N, 5.8. Mass Spec. (EI): 689 $(M)^+$. IR (cm^{-1}): ν 2960 w, 2912 w, 2866 w, 2253 w, 1614 m, 1598 m, 1577 m, 1535 m, 1474 m, 1416 m, 1385 m, 1351 w, 1316 w, 1216 w, 1241 w, 1200 m, 1165 m, 1095 w, 1029 w, 907 s, 815 w, 788 w, 732 w, 665 s, 650 s. EPR (toluene, 298 K): $g_{iso} = 1.98$, $A_{iso} = 94$G, (toluene, 40 K) $g_\perp = 1.96$, $A_\perp = 169$ G, $g_{||} = 1.99$, $A_{||} = 60$ G, $\mu_{eff} = 1.76\ \mu_B$.

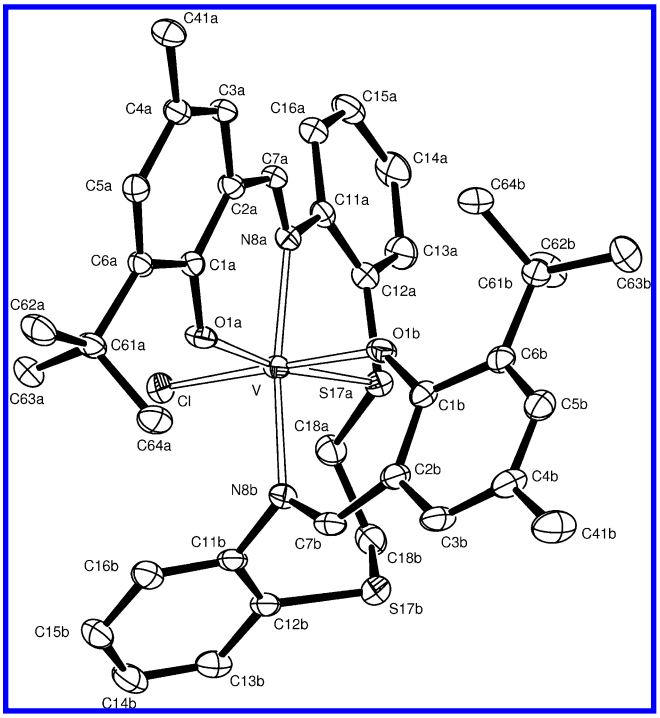

Figure 4. View of a molecule of **3** showing the atom numbering scheme. Thermal ellipsoids are drawn at the 50% probability level.

Scheme 3. Proposed Mechanism for C−S Bond Cleavage[55]

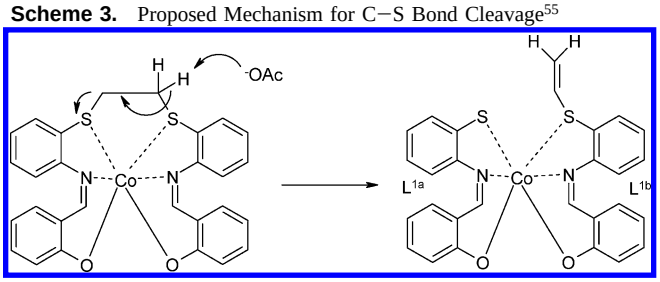

2.2.2. Preparation of [V(N*p*-tol)L^1] (2). As described above for **1**, but using [V(N*p*-tol)(OEt)$_3$] (0.51 g, 1.76 mmol) and $\mathbf{H_2L^1}$ (1.00 g, 1.60 mmol) to give **2** as a brown solid. Yield 0.79 g, 63% Mp decomposed at 103 °C. Anal. Found: C, 69.4; H, 6.3; N, 5.4. $C_{45}H_{49}N_3O_2S_2V$ requires: C, 69.5; H, 6.5; N, 5.6. Mass Spec. 778 $(M)^+$, 689 $(M-C_7H_7)^+$. IR (cm^{-1}): ν 1615 m, 1588 m, 1537 m, 1499 w, 1417 m, 1014 s, 928 m, 858 m, 800 s, 757 w. EPR (toluene, 298 K): $g_{iso} = 1.98$, $A_{iso} = 95$ G, (toluene, 40 K) $g_\perp = 1.96$, $A_\perp = 168$ G, $g_{||} = 1.99$, $A_{||} = 58$ G, $\mu_{eff} = 1.63\ \mu_B$.

2.2.3. Preparation of [V(Cl)L^1] (3). (a). As for **1**, but using [V(O)(O*n*-Pr)$_3$] (0.40 mL, 1.76 mmol), $\mathbf{H_2L^1}$ (1.00 g, 1.60 mmol), and dimethylaluminum chloride (1.76 mL, 1.0 M, 1.76 mmol) to give dark-brown blocks of **3**. Yield 0.89 g, 78%.

(b) As for **1**, but using [$VCl_3\cdot$3THF] (0.66 g, 1.76 mmols) and $\mathbf{H_2L^1}$ (1.00 g, 1.60 mmol) to give deep-red blocks of **3**. Yield 1.05 g (93%). Mp 195 °C. Anal. Found: C, 63.9; H, 6.1; N, 5.0. $C_{38}H_{42}ClN_2S_2O_2V\cdot{}^1/_2$MeCN requires: C, 64.2; H, 6.0; N, 4.8. Mass Spec. (MALDI): 709 $(M)^+$. IR (cm^{-1}): ν 2359 m, 2330 m, 1533 s, 1398 m, 1261 m, 1231 s, 1203 s, 1165 s, 1092 m, 1018 m, 866 s, 800 m, 667 m. $\mu_{eff} = 2.52\ \mu_B$.

2.2.4. Preparation of [V(O)L^2] (4). As for **1**, but using [V(O)-(O*n*-Pr)$_3$] (0.39 mL, 1.72 mmol) and $\mathbf{H_2L^2}$ (1.00 g, 1.57 mmol), giving **4** as a brown solid. Yield 0.93 g, 84% Mp decomposed at 148 °C. Anal. Found: C, 67.0; H, 6.5; N, 3.9. $C_{39}H_{44}N_2O_3S_2V$ requires: C, 66.6; H, 6.3; N, 4.0. Mass Spec. 704 $(M)^+$. IR (cm^{-1}): ν 1615 m, 1533 w, 1261 s, 1093 bs, 1020 bs, 864 m, 800 s. EPR

Table 3. Selected Bond Lengths (Ångstroms) and Angles (Degrees) for **7**

V(1)−O(1A)	1.915(7)	V(1)−N(1B)	2.061(8)
V(1)−O(1B)	1.876(6)	V(1)−S(1A)	2.367(3)
V(1)−N(1A)	2.104(8)	V(1)−S(1B)	2.559(3)
O(1A)−V(1)−N(1A)	88.3(3)	O(1B)−V(1)−N(1B)	90.8(3)
O(1A)−V(1)−N(1B)	97.5(3)	O(1B)−V(1)−S(1B)	170.9(2)
O(1A)−V(1)−S(1A)	162.3(2)	N(1A)−V(1)−N(1B)	171.3(3)
O(1A)−V(1)−S(1B)	84.6(2)	S(1A)−V(1)−S(1B)	80.74(10)
O(1A)−V(1)−O(1B)	94.0(3)		

Table 4. Ethylene Polymerization Runs for **1**−**7**

catalyst	weight[a]	activity[b]	M_w	M_n	P.D.I.	M.P.[c]
1	0.65	2580	246 000	84 500	2.9	137.6
2	1.44	5744	183 000	45 500	4.0	135.2
3[d]	1.86	11 130	213 000	57 900	3.7	134.6
4[e]	1.60	7675	244 000	77 900	3.1	134.3
5	1.53	6108	256 000	105 000	2.5	137.3
6	0.26	1052	160 000	67 900	2.4	134.1
7	1.03	2068	207 000	61 600	3.4	134.4
8[f]	1.36	10 880	98 700	40 300	2.5	134.6
9[f]	1.00	8000	155 000	48 700	3.2	134.2

[a] Polymer weight in grams. [b] Units: g/mmol vanadium·hr·bar. [c] Degrees Celcius, measured by DSC. [d] Run time of 20 min. [e] Run time of 25 min. [f] Run time of 15 min. All runs were completed with 0.5 μmol of vanadium, 4000 equiv of DMAC, and 0.1 mL of ETA in 50 mL of toluene at 60 °C for 30 min.

(toluene, 298 K): $g_{iso} = 1.99$, $A_{iso} = 98$ G, (toluene, 40 K), $g_\perp = 1.95$, $A_\perp = 173$ G, $g_\parallel = 1.99$, $A_\parallel = 61$ G, $\mu_{eff} = 1.42\ \mu_B$.

2.2.5. Preparation of [V(O)L^3] (5). As for **1** but using [V(O)(O*n*-Pr)$_3$] (0.38 mL, 1.69 mmol) and **H$_2$L^3** (1.00 g, 1.53 mmol), giving **5** as dark-brown blocks. Yield: 0.47 g (42%). Mp > 250 °C. Anal. Found: C, 67.0; H, 6.5; N, 3.9. $C_{40}H_{46}N_2O_3S_2V$ required: C, 67.0; H, 6.5; N, 3.9. Mass Spec. (MALDI): 717 $(M)^+$. IR (KBr, cm^{-1}): ν 1611 m, 1592 m, 1533 m, 1308 m, 1262 m, 1238 m, 1200 m, 1172 m, 1102 m, 1067 m, 1021 m, 994 m, 928 m, 854 m, 803 m, 749 w, 737 w. EPR (toluene, 298 K): $g_{iso} = 1.99$, $A_{iso} = 98$ G, (toluene, 40 K), $g_\perp = 1.95$, $A_\perp = 175$ G, $g_\parallel = 1.99$, $A_\parallel = 61$ G, $\mu_{eff} = 1.35\ \mu_B$.

2.2.6. Preparation of [VL^4] (6). A solution of [V(O)(O*n*-Pr)$_3$] (0.40 mL, 1.75 mmol) and **H$_2$L^4** (1.00 g, 1.59 mmol) in diethyl ether (30 mL) was stirred at room temperature for 15 min, after which the solvent was removed in vacuo. A further portion of diethyl ether (30 mL) was added, and the solution was stirred for 15 min. This process was repeated 5 times, after which the solid residue was extracted into warm dichloromethane (30 mL) and filtered. Removal of the solvent in vacuo gave **6** as a brown solid. Yield 0.74 g, 67% Mp 118−120 °C. Anal. Found: C, 66.0; H, 6.4; N, 3.8. $C_{38}H_{44}N_2O_2S_2V\cdot{}^1/_4CH_2Cl_2$ requires: C, 65.7; H, 6.7; N, 4.0. Mass Spec. 676 $(M)^+$. IR (cm^{-1}): ν 2361 w, 1574 m, 1537 m, 1305 m, 1261 s, 1239 m, 1200 m, 1167 m, 984 m, 937 w, 860 m, 802 s, 750 m, 731 m, 669 w. EPR (toluene, 298 K): $g_{iso} = 1.98$, $A_{iso} = 97$ G, (toluene, 40 K) $g_\perp = 1.96$, $A_\perp = 168$ G, $g_\parallel = 1.99$, $A_\parallel = 60$ G, $\mu_{eff} = 1.36\ \mu_B$.

2.2.7. Preparation of [VL′] (7). (i) [V(O)(O*n*-Pr)$_3$] (0.24 mL, 1.06 mmol) and **H$_2$L^4** (1.00 g, 1.59 mmol) were combined in a Schlenk flask. Toluene (40 mL) was added, and the solution was refluxed for 24 h. On cooling, the solvent was removed in vacuo, and the residue extracted into either warm acetonitrile (40 mL) or diethyl ether (40 mL). Prolonged standing at room temperature gave dark-brown blocks of **7**. Yield 580 mg (83%). Mp decomposes at ∼161 °C. Anal. Found: C, 67.5; H, 6.2; N, 4.3. $C_{74}H_{80}O_4S_4N_4V_2$ requires: C, 67.4; H, 6.1; N, 4.3. Mass Spec. (MALDI): 971 $(M-[SC_6H_4NCH\text{-}3\text{-}Me\text{-}5\text{-}{}^tBuC_6H_2O]-V)^+$, 645 $(M-2[SC_6H_4NCH\text{-}3\text{-}Me\text{-}5\text{-}{}^tBuC_6H_2O]-V)^+$, 624 (ligand **H$_2$L^1**)$^+$ IR (cm^{-1}): ν 2730 w, 2347 w, 1595 s, 1575 m, 1536 s, 1419 m, 1353 m, 1305 m, 1261 s, 1202 m, 1168 m, 938 w, 904 w, 859 m, 798 s, 755 s, 732 w, 687 w, $\mu_{eff} = 2.50\ \mu_B$.

2.3. Crystallographic Analysis. For each sample, a crystal was mounted in oil on to a glass fiber and fixed in a cold nitrogen stream, on either a Bruker-Nonius Kappa CCD diffractometer (for crystal **1**) or an Oxford Diffraction Xcalibur-3 CCD diffractometer (for all other samples); both systems were equipped with Mo Kα radiation ($\lambda = 0.71073$ Å) and a graphite monochromator. In all of the cases, intensity data were measured by thin-slice ω- and φ-scans. Data were processed using the CrysAlis-CCD and −RED[49] programs or, for **1**, the *DENZO*/*SCALEPACK*[50] programs, with absorption corrections applied in *SADABS*.[51] The structures were determined by the direct methods routines in the *SHELXS* program[51] and refined by full-matrix least-squares methods, on F^2's, in *SHELXL*.[52] The non-hydrogen atoms were refined with anisotropic thermal parameters. In **H$_2$L^1** and **H$_2$L^4**, the phenolic hydrogen atoms were located in difference maps and were refined freely; all of the other hydrogen atoms in all of the samples were included in idealized positions, and their U_{iso} values were set to ride on the U_{eq} values of the parent carbon atoms. Scattering factors for neutral atoms were taken from reference.[53] Crystal data and refinement results are collated in Table 1. Computer programs used in this analysis have been noted above and were run through *WinGX*[54] on a Dell Precision 370 PC at the University of East Anglia.

2.4. Ethylene Polymerization Procedure. Ethylene polymerizations were performed in a flame-dried glass flask (250 mL) equipped with a magnetic stirrer bar. The flask was evacuated and filled with ethylene gas at 1 bar, which was maintained throughout the polymerization. The flask was further purged several times with ethylene, and then 50 mL of dry, degassed toluene was added via a glass syringe. If applicable, the reactivating agent ETA was added (0.1 mL, 0.72 mmol) at this stage. The solution was then stirred for 10 min to allow ethylene saturation, and the correct temperature was acquired via the use of a water bath. The cocatalyst was added, and the solution was stirred for a further 5 min. The procatalyst was injected as a toluene solution (stock solutions of 1 μmol mol^{-1} were prepared immediately prior to use). The polymerization time was measured from procatalyst injection; the polymerization was quenched by the injection of 5 mL of methanol. The resulting polymer was transferred into a 500 mL beaker containing acidified methanol, and the solid polyethylene was collected via filtration and dried at 90 °C overnight.

2.5. Ethylene/1-Hexene Polymerization. Copolymerizations were performed in a flame-dried glass flask (250 mL) equipped with a magnetic stirrer bar. The flask was evacuated and filled with ethylene gas at 1 bar, which was maintained throughout the polymerization. The flask was further purged several times with ethylene and then 40 mL of dry, degassed toluene was added via

(49) *CrysAlis-CCD* and *-RED*, Oxford Diffraction Ltd.: Abingdon, U.K., 2005.
(50) Otwinowski, Z.; Minor, W. Processing of X-ray Diffraction Data Collected in the Oscillation Mode. In *Methods in Enzymology*, Macromolecular Crystallography, Part A; Carter, C. W., Jr., Sweet, R. M., Eds.; Academic Press: New York, 1997; Vol. 276, pp 307−326.
(51) Sheldrick, G. M. *SADABS: Program for Calculation of Absorption Corrections for Area-Detector Systems*, version 2.10; Bruker AXS Inc.: Madison, WI, U.S.A., 2003.
(52) Sheldrick, G. M. *SHELX-97: Programs for Crystal Structure Determination (SHELXS) and Refinement (SHELXL)*; University of Göttingen: Göttingen, Germany, 1997.
(53) *International Tables for X-ray Crystallography*; Kluwer Academic Publishers: Dordrecht, The Netherlands, 1992; Vol. C, pp 500, 219, and 193.
(54) Farrugia, L. J. *J. Appl. Crystallogr.* **1999**, *32*, 837.

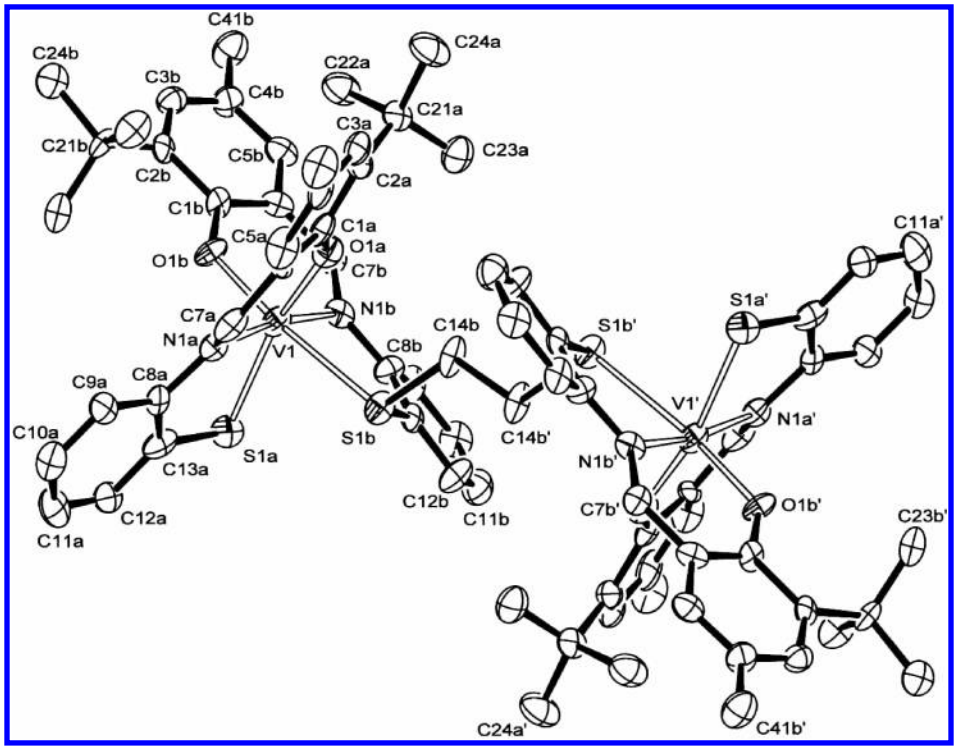

Figure 5. View of a molecule of **7** showing the atom numbering scheme. Thermal ellipsoids are drawn at the 50% probability level.

Scheme 4. Representation of the New Procatalysts **1**−**7** and the Known Phenoxy-imine (F.I.) Procatalysts **8** and **9** [46]

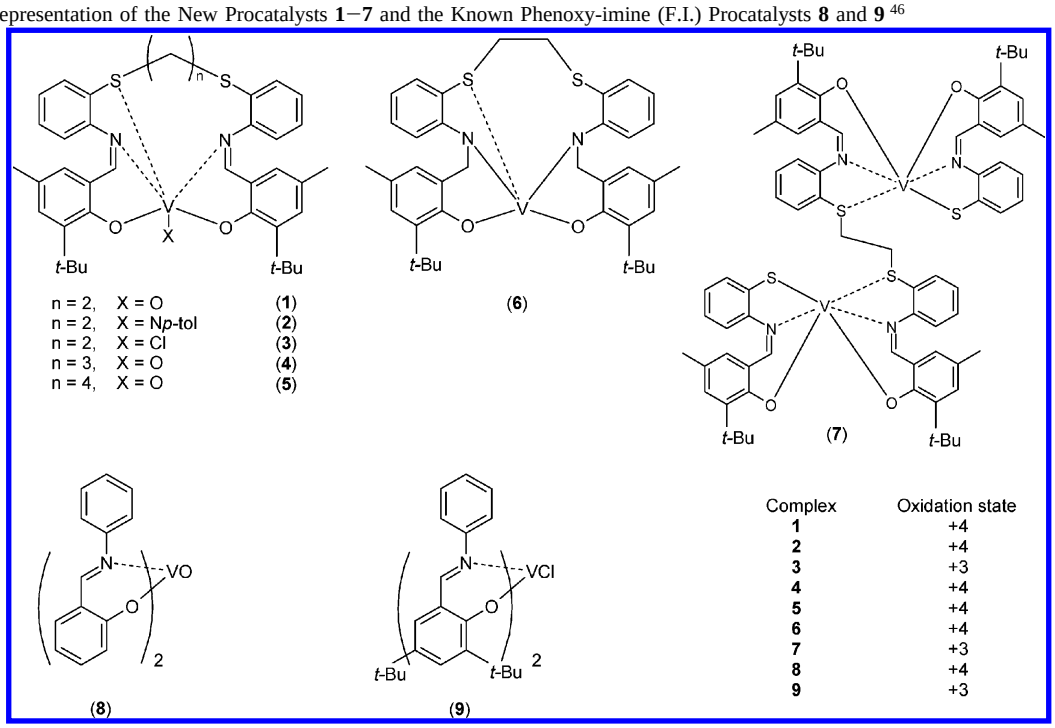

a glass syringe. The reactivating agent, ETA, was added (0.1 mL, 0.72 mmol) along with 1-hexene (5 mL, 4000 equiv). The solution was then stirred for 10 min, to allow ethylene saturation, and the correct temperature was acquired via the use of a water bath. DMAC (4 mL, 1M solution, 400 equiv) was added via a glass syringe, and the solution was stirred for a further 5 min. The procatalyst was injected as a toluene solution (stock solutions of 1 μmol mL^{-1} were prepared immediately prior to use). The polymerization time was set at 30 min, after which the reaction was quenched by the injection of 5 mL of methanol. The resulting polymer was transferred into 500 mL of acidified methanol, and the precipitate was collected via filtration and dried at 90 °C overnight.

3. Results and Discussion

3.1. Synthesis and Structure of Proligands H_2L^1−H_2L^4. The proligand H_2L^1 was readily synthesized in good yield (73%) via an adaptation of the method reported by Rajeskhar et al.[55] The reaction of 1,2-bis(2-aminophenylthio)ethane (**A**) in a 1:2 ratio with 3-Me-5-*t*-Bu-salicaldehyde in refluxing

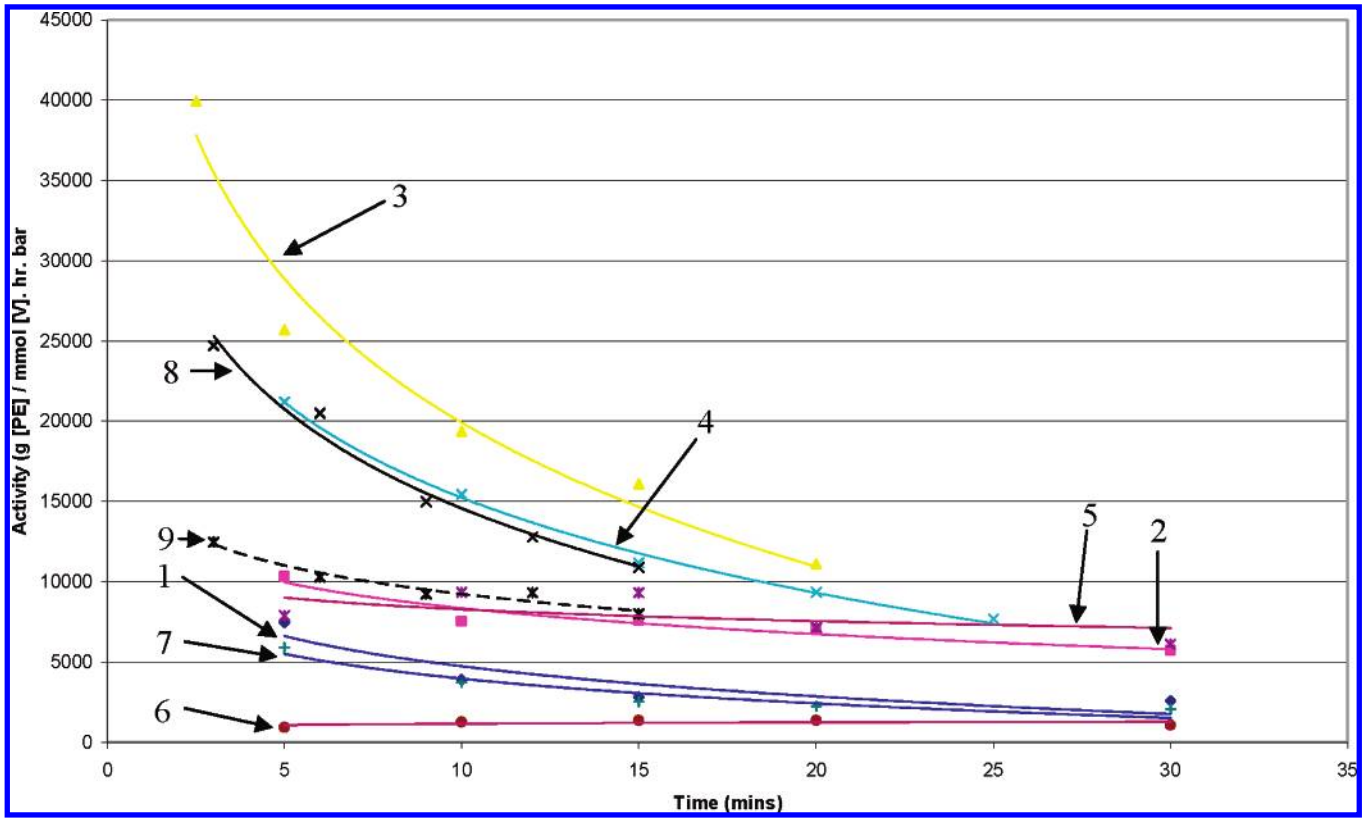

Figure 6. Lifetime graph of ethylene polymerization for **1**−**7**. Conditions: 50 mL toluene at 60 °C, 0.1 mL ETA, 4 000 equiv DMAC, 0.5 μmol of vanadium.

ethanol produced $\mathbf{H_2L^1}$ as a pure (by ^{1}H NMR) orange solid. X-ray quality crystals were grown from a saturated ethanol solution upon slow evaporation of the solvent. A molecule of proligand $\mathbf{H_2L^1}$ is depicted in part a of Figure 1.

The molecule has C_i symmetry, with the center of inversion between C18 and C18′. The phenoxy-imine moieties are close to planar and linked via the bridging ArS−C_2H_4−SAr group. The planarity of the phenoxy-imine group is aided by a single hydrogen bond from the phenolic OH to the nitrogen of the imine group [H(1)···N(8) bond length of 1.82(3) Å with a corresponding O(1)−H(1)···N(8) angle of 156(3)°]. The torsion angle about the S(17)−C(18) bond, 169.49(15)°, indicates an anti arrangement of the phenoxy-imine moiety. Most of one-half of the molecule forms a good mean-plane; the other half forms a parallel plane, which is removed by a step (perpendicular distance 3.040 Å) through the S−CH_2−CH_2−S link. Either side of the first plane, there are overlapping planes of adjacent molecules, related by *a*-glide symmetry. Hence, a series of half-molecule planes, spaced along the *a* axis, slot between a neighboring series of symmetry-related planes (part b of Figure 1). The angle between the normals of neighboring planes is 11.64(4)°, and the distance between these planes is ca. 3.45 Å.

The reduction of the imine moieties of $\mathbf{H_2L^1}$ is facile at room temperature in THF using 2 or more equiv of $LiAlH_4$ per imine (isolated yield of $\mathbf{H_2L^4}$, 82%). The complete formation of $\mathbf{H_2L^4}$ can easily be monitored by the loss of the initial bright-orange coloration (indicating the presence of $\mathbf{H_2L^1}$) and the appearance of a clear pale-yellow solution. Crystals suitable for X-ray crystallography were obtained on slow cooling of a warm, saturated acetonitrile solution to ambient temperature. The molecular structure of $\mathbf{H_2L^4}$ is given in Figure 2.

The molecule is centrosymmetric; however, unlike $\mathbf{H_2L^1}$, the phenoxy-amine moiety is not planar because of the reduction of the imine groups leading to increased flexibility around the C−N bond and the formation of a weaker hydrogen bond [H1a···N1 2.11(4) Å with an O1a−H1a··· N1 angle of 148(3)°]. There is additional hydrogen bonding [H(1)···S(1) 2.63 Å with N(1)−H(1)···S(1) at 108°] to the bridging thioether group; this further affects the conformation of the $\mathbf{H_2L^4}$. Rather than adopting an anti arrangement as previously seen in $\mathbf{H_2L^1}$, the torsion angle C(14′)−C(14)−S(1)−C(13) [68.6(3)°] indicates that the phenoxy-amine moiety adopts a gauche conformation. A difference in the packing is also observed (part b of Figure 2) with no overlap of extended planar moieties. Only van der Waals interactions are observed intermolecularly.

The length of the ethane bridge can be readily varied by selection of the appropriate dibromoalkane precursor (Scheme 2). The propane- ($\mathbf{H_2L^2}$) and butane- ($\mathbf{H_2L^3}$) bridged molecules were isolated (and characterized) as yellow oils in 84 and 40% yield, respectively. Both are highly soluble in hydrocarbon solvents, and in the case of $\mathbf{H_2L^3}$, trituration with hexane afforded a yellow solid.

(55) Rajsekhar, G.; Rao, C. P.; Saarenketo, P.; Nattinen, K.; Rissanen, K. *New J. Chem.* **2004**, *28*, 75.

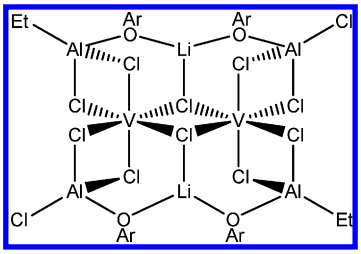

Figure 7. Example of V−Cl−Al motif postulated as an active species in vanadium-based α-olefin polymerization.

3.2. Synthesis and Structure of 1−7. The reaction of $\mathbf{H_2L^1}$ with [VO(O*n*-Pr)$_3$] in refluxing toluene affords, following work up, brown block crystals of [V(O)L^1] (**1**) in good yield (ca. 70%). Crystals suitable for single-crystal X-ray analysis were obtained from a saturated acetonitrile solution upon prolonged standing (2−3 days) at ambient temperature. The molecular structure of **1** is shown in Figure 3, with selected bond lengths and angles given in Table 2. Because of the constrained nature of the ligand, the binding of the salicylaldimine groups is such that the nitrogens are bound trans [N1B−V−N1A 164.93(7)°] with respect to each other, with the oxygens being bound in the cis fashion [O1A−V−O1B 91.24(6)°]. The binding of the vanadyl oxygen atom and one of the bridging thioether groups completes the pseudo-octahedral geometry of the vanadium(IV) center. The V−O [1.9209(14) and 2.0294(14) Å] and V−N [2.0883(16) and 2.1037(16) Å] bond distances are typical of values observed previously for vanadium phenoxy-imine complexes,[17] whereas the V−S bond distance [2.5252(6) Å] is slightly shorter than that observed in [VL$^S{}_2$] [2.5306(4) Å] [L$^S{}_2$ = 2,2′-S{4,6-(*t*-Bu)$_2$C$_6$H$_2$O}$_2$].[56] The vanadyl V=O bond length, 1.6193(4) Å, is typical[53] and gives a strong absorption in the IR spectrum at υ 1029 cm^{-1}.

A similar reaction of $\mathbf{H_2L^1}$ with [V(N*p*-tol)(OEt)$_3$] produced the imido analogue of **1**, namely [V(N*p*-tol)L$_1$] (**2**), as characterized by elemental analysis, mass spectrometry, EPR, and magnetic moment. Reaction of $\mathbf{H_2L^1}$ with [V(O)(O*n*-Pr)$_3$] in the presence of excess DMAC, led to isolation of the vanadium(III) complex [V(Cl)L^1] (**3**) in ca. 90% yield. Crystals suitable for an X-ray diffraction study were isolated from a saturated solution of acetonitrile on standing at ambient temperature for 7 days. A molecule of **3** is shown in Figure 4 (selected bond lengths and angles are given in Table 2) and is found to be essentially isostructural to that of **1**.

The V−Cl bond length [2.3717(6) Å] is slightly longer than that found in previously reported vanadium(III) complexes [2.227(1) to 2.2923(16) Å],[58,59] possibly due to the presence of three dative bonds increasing the electron density at the metal center. The presence of the chlorine atom was verified empirically using a standard halide test with AgNO$_3$. An effective magnetic moment of 2.52 μ_B (Evans' method), consistent with a vanadium(III) (d^2) high-spin system was observed; the spin-only value is 2.83 μ_B, with the large deviation attributed to the possible contribution of orbital angular momentum possible in 3d^2 systems, but is comparable with other vanadium(III) complexes (e.g., 2.52 μ_B for [V(OC$_6$H$_2$(CH$_2$NMe$_2$)$_2$-2,6-Me-4)$_3$]).[59] **3** can also be synthesized by refluxing [VCl$_3$·3THF] and $\mathbf{H_2L^1}$ in toluene, with the loss of 2 equiv of HCl. After workup and prolonged standing at ambient temperature (2−3 weeks), red rectangular crystals of **3** as the acetonitrile solvate formed in good yield (78%).

Table 5. Ethylene Screening for **1**

run	cocatalyst	cocatalyst equiv	T[a]	weight[b]	activity[c]	M_w	M_n	P.D.I.
1	DMAC	2000	0	0.049	196	340 000	112 000	3.0
2	DMAC	2000	25	0.103	412			
3	DMAC	2000	45	0.118	472	229 000	78 900	2.9
4	DMAC	2000	60	0.597	2388			
5	DMAC	2000	80	0.044	176	75 300	13 700	5.5
6	DMAC	1000	25	0.474	1896	482 000	227 000	2.1
7	DMAC	2000	25	0.501	2004			
8	DMAC	3000	25	0.562	2248	439 000	204 000	2.2
9	DMAC	4000	25	0.475	1900			
10	DMAC	5000	25	0.431	1724	445 000	206 000	2.2
11	MAC	2000	25	0.696	2784	420 000	142 000	3.0
12	MAC[d]	2000	25	0.824	3296	308 000	62 500	4.9
13	DMAC	2000	25	0.103	412	489 000	205 000	2.4
14	DMAC[d]	2000	25	0.101	406	595 000	270 500	2.2
15	TMA	2000	25					
16	TMA[d]	2000	25					
17	MAO	2000	25					
18	MAO[d]	2000	25					

[a] Degrees Celcius. [b] Polymer weight in grams. [c] Units: g/mmol vanadium·hr·bar. [d] Without ETA. All runs were completed with 1 μmol of vanadium and 0.1 mL of ETA in 50 mL of toluene for 30 min.

4 and **5** being the vanadyl-bearing propane-bridged and butane-bridged analogues, respectively, were prepared as described for **1**; however, high solubility in common organic solvents has, to-date, thwarted attempts to obtain crystals suitable for single-crystal X-ray diffraction.

The vanadium ethane-bridged amine complex, **6**, was ultimately isolated in good yield (67%) under less-forcing conditions than previously employed for **1**−**5**. It was found that the reaction could be driven at room temperature in diethyl ether by repeatedly stirring for 15 min, followed by the removal in solvent in vacuo. Over four or five cycles, a deep red/brown coloration developed, at which point the crude material was extracted into dichloromethane. A binding motif similar to that seen in **1** and **3** is tentatively suggested, whereby both phenolate groups are bound to the metal center, as well as in this case, both amine nitrogens; the presence of a vanadium−sulfur interaction cannot be directly proven in the absence of a crystal structure determination. The vanadium center has no extra functionality by way of a bound oxygen atom (i.e., no vanadyl group); the magnetic moments and EPR results providing corroborating evidence for the presence of a d^1 vanadium(IV) species. The mass spectrum for this compound displays a peak at 676, which can be attributed to the molecular ion peak for the above suggested structure (see also Scheme 4); however, without conclusive

(56) Chaudhuri, P.; Paine, T. K.; Weyhermuller, T.; Slep, L. D.; Neese, F.; Bill, E.; Bothe, E.; Wieghardt, K. *Inorg. Chem.* **2004**, *43*, 7324.
(57) Redshaw, C.; Rowan, M. A.; Warford, L.; Homden, D. M.; Arbaoui, A.; Elsegood, M. R. J.; Dale, S. H.; Yamato, T.; Casas, C. P.; Matsui, S.; Matsuura, S. *Chem. Eur. J.* **2007**, *13*, 1090.
(58) Berreau, L. M.; Hays, J. A.; Young, V. G.; Woo, L. K. *Inorg. Chem.* **1994**, *33*, 105.
(59) Hagen, H.; Boersma, J.; Lutz, M.; Spek, A. L.; van Koten, G. *Eur. J. Inorg. Chem.* **2001**, 117.

Table 6. Ethylene/1-Hexene Copolymerization Results

run	catalyst	1-hexene equiv	weight[a]	activity[b]	C_6 = mol %[c]	M_w	M_n	P.D.I.
1	**1**	400	1.16	230		88 100	39 400	2.2
2	**1**	800	1.01	200				
3	**1**	1600	0.82	164				
4	**1**	2400	0.42	85				
5	**1**	3200	0.41	82	7.3			
6	**1**	4000	0.22	43	11.3	39 800	21 000	1.9
7	**1**	4800	0.14	28	13.6			
8	**1**	5600	0.11	21	11.8			
9	**1**	6400	0.18	36	12.1			
10	**1**	7200	0.21	42	11.6	21 000	10 800	1.9
11	**1**	8000						
12	**2**	4000	2.58	516	6.3	38 100	19 200	2.0
13	**3**	4000	3.31	662	8.4	41 700	19 000	2.2
14	**4**	4000	5.95	1190	5.9	24 400	8 520	2.9
15	**5**	4000	2.86	572	8.3	36 900	18 900	2.0
16	**6**	4000	1.48	148	5.1	62 800	33 300	1.9
17	**7**	4000	1.22	244	7.6	47 000	23 000	2.0
18	**1**	4000	4.35	870	13.0	39 800	21 000	1.9
19[d]	**1**	4000	0.44	89	10.2	5780	2980	1.9

[a] Polymer weight in grams. [b] Units: g/mmol vanadium·hr·bar. [c] Calculated by ^{1}H NMR. [d] $T = 45$ °C. All runs completed with 10 μmol of vanadium, 0.1 mL of ETA, 400 equiv of DMAC and 40 mL of toluene at 25 °C for 30 min.

X-ray data, the possibility of a bridging dinuclear species similar to that of **7** or an amido-hydroxo species cannot be completely ruled out.

The reaction between $\mathbf{H_2L^4}$ and [V(O)(O*n*-Pr)$_3$] in refluxing toluene, following extraction into hot acetonitrile, gave brown crystals of **7** in 19% yield. Single-crystal X-ray analysis of the complex (Figure 5) unexpectedly revealed the binding of two metal centers to one $S_2N_2O_2$ molecule, with the meridonal binding of an SNO group to each vanadium center (Scheme 4, **7**). Additionally, each vanadium atom is coordinated, also meridonally, through the SNO atoms by a thiolate ligand produced by the cleavage of an $\mathbf{H_2L^1}$ molecule. Selected bond lengths and angles for **7** are given in Table 3.

An analogous ligand to the parent ligand $\mathbf{H_2L^4}$ has recently been shown to undergo cleavage of one of the C−S bonds for a cobalt(II) system (Scheme 3).[55]

We invoke a similar mechanism for **7**; however, in the case of **7**, the fragment $\mathbf{L^{1b}}$ (see Scheme 3) does not appear in the isolated product **7**. Rather, this product is the result of the combination of two [$\mathbf{L^{1a}}$V]-type fragments, which are bound by an intact $\mathbf{L^1}$ ligand. We have not be able to isolate (or identify) other products in this reaction. The reformation of the imine arms in **7** is most likely driven by the reductive elimination of dihydrogen and water.

In light of the characterization of **7**, the stoichiometry of the reaction was altered accordingly such that the reaction involving [V(O)(O*n*-Pr)$_3$] and $\mathbf{H_2L^4}$ was carried out in a 2:3 (metal/ligand) ratio, resulting in the isolation of the desired product **7** in good yield (83%).

As in the proligands $\mathbf{H_2L^1}$ and $\mathbf{H_2L^4}$, **7** contains a center of symmetry at the midpoint of the ethane bridge (between C14b and C14b′). The vanadium centers are pseudo octahedral, each with two phenolate bonds, to O(1A) and O(1B), three dative bonds, to N(1A), N(1B), and S(1B), and a thiolate bond to S(1A). The V−S dative bond is comparable to that found in **1**. The complex displayed a magnetic moment of 2.50 μ_B, which is consistent with a vanadium(III) system (vide infra). In contrast to **3**, **7** is highly unstable, producing a high degree of fragmentation when analyzed using mass spectrometry, and only a very weak signal for the molecular ion is observed; peaks due to the loss of ligands around the metal centers dominate.

3.3. Polymerization Results. 3.3.1. Ethylene Homopolymerization. Procatalysts **1**−**7** (Scheme 4) were screened for α-olefin polymerization in the presence of a variety of organoaluminum cocatalysts, namely, methylaluminoxane (MAO), trimethylaluminum (TMA), methylaluminum dichloride (MAC), and dimethylaluminum chloride (DMAC). In the presence of DMAC and the reactivating agent ETA, **1**−**7** exhibited very good activities (>1000 g/mmol·h·bar) for ethylene polymerization as defined by the Gibson criteria.[3] Lifetime studies (Table 4 and Figure 6) carried out upon systems **1**−**7** as well as the known **8** and **9**, showed in general, a steady decrease in catalytic activity over the first 15 min period (up to 50% reduction in activity). The lower level of activity is maintained throughout the polymerization screening lifetime (∼30 min). Only in the case of **3** was there a pronounced decrease in catalytic activity, where initial values of ca. 40 000 g/mmol·h·bar at 5 min fell sharply to around 11 000 g/mmol·h·bar at ca. 15 min; again this lower activity is maintained throughout the remainder of the polymerization run. The greater activity observed by **3** could be attributed to the lower oxidation state of the vanadium center, a theory supported by Allegra et al.[60] In the case of **7**, the instability of the complex is thought to produce lower activities observed when compared to those of **3**. All of the polymers produced using **1**−**7** were of high molecular weight (M_w = 160 000−256 000) with narrow polydispersity indexes (2.4−4.0) with melting points of 134−138 °C being typical of values for linear polyethylene. Under analogous polymerization conditions, the known **8** and **9** also displayed very good activities. In particular, vanadium(IV) complex **8**

(60) Zambelli, A.; Allegra, G. *Macromolecules* **1980**, *13*, 42.

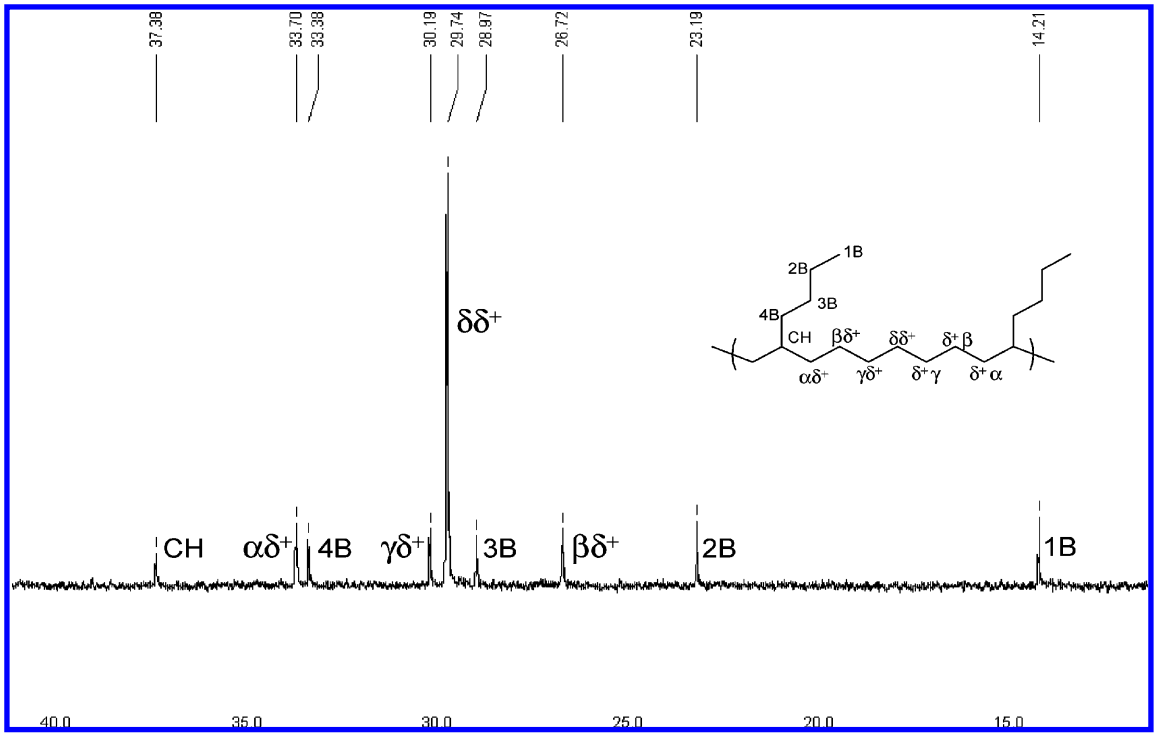

Figure 8. ^{13}C NMR ($CDCl_3$) of ethylene/1-hexene copolymer using procatalyst **1**.

upon activation with DMAC afforded a system with a catalytic activity of ca. 10 500 g/mmol·h·bar; cf. 8 000 under analogous conditions using **9**. The activity of some of the catalysts was such that mass transport problems were encountered, leading to the shorter runs times quoted; however, from these results it is interesting to note that although the vanadium(IV) species from procatalysts **1**−**7**, notably **4**, give activities comparable to that of **8**, the vanadium(III) procatalysts **3** and **9** give quite different activities. This suggests that additional π donation from the sulfur atom in **3** helps to stabilize the lower oxidation state, producing the higher activity. However, any structure−activity relationship discussions are best restricted to the procatalyst because the exact nature of the active species in these vanadium-based systems still remains a mystery.

Recent studies have shown that the nature of the cocatalyst is crucial for vanadium-based polymerization catalysis.[16,17] Here, the use of alkyl aluminum compounds (TMA and MAO; Table 5, runs 15 and 17) with **1** led to negligible activites, whereas the chlorinated cocatalysts (MAC and DMAC; Table 5, run 11 vs run 13) produced moderate-to-high activities. The use of DMAC as a cocatalyst in combination with **3** produced the highest activity (ca. 11 000 g/mmol·h·bar). The necessity of a chloro-organoaluminum cocatalyst is supported by the work of Gambarotta et al.,[6] who have postulated that the catalytically active species in vanadium-based α-olefin polymerization utilizes bridging chloro groups in V−Cl−Al-type motifs (Figure 7). In no instance here was any polymer produced in the absence of an aluminum cocatalyst, and the cocatalyst alone produced only negligible polymer.

Maximum catalytic activities for **1** were observed at ca. 60 °C (Table 5, runs 1−5), and, as previously found in vanadium-based ethylene catalysis,[16] the increase in polymerization temperature resulted in a decrease in the molecular weight of the polyethylene and broader polydispersity. A significant decrease in the molecular weight was observed with **8** (M_w = 98 700) compared to molecular weights produced by the other vanadium(IV) procatalysts herein; upon increasing the temperature to 80 °C, a further decrease in molecular weight was observed (M_w = 37 900) and also a broadening of the range of molecular weights (P.D.I. increases from 3.5 to 17) indicating the presence of more than one active species, while also displaying the thermal instability of the active species. **9**, a vanadium(III) system, faired better under the same conditions, producing a polymer with a narrow distribution (P.D.I. in the range 2.3−3.4) even at elevated temperature. However, an even more-drastic decrease in molecular weight was observed from M_w = 155 000 at 60 °C to M_w = 13 400 at 80 °C.

A maximum in activity is also observed with varying cocatalyst concentration (Table 5, runs 6−10), with 3 000 equiv producing the highest activity ([Al:V] range = 1000−5000). However, the influence of the Al:V ratio is not dramatic; the lowering of the Al:V ratio to 1 000 equiv (run 6) still produced a highly active polymerization system. Unlike previously observed for more-active vanadium systems, the removal of ETA from the polymerization system (Table 5, runs 11 vs 12) did not result in a dramatic change in activity; however, it did lead to a broadening of the P.D.I. of the polymers, suggesting its role herein to be that of maintaining a single active species.

Within the vanadyl family of catalysts presented here (**1**, **4**, and **5**), there is no clear trend for activity on increasing the length of the backbone. The lowest activity is exhibited by procatalyst **1**, for which n = 2, with procatalyst **4** (n = 3) affording the highest activity, whereas **5** (n = 4) falls

between **1** and **4**. After $t = 25$ min, the activities of **4** and **5** are comparable.

3.3.2. Ethylene/1-Hexene Copolymerization. To date, the use of vanadium-based complexes for the copolymerization of α-olefins is somewhat limited. Recent investigations have examined the vanadium-catalyzed copolymerization of ethylene-propylene,[61] ethylene-norbornene, and ethylene/1-alkenes.[15,62,63]

Procatalysts **1**−**7** in the presence of DMAC catalyze the polymerization of ethylene/1-hexene with activities, levels of incorporation, molecular weights, and polydispersities all within a narrow range (Table 6), suggestive of single-site catalysis and a common active species. The highest activity (run 14), ca. 1 200 g/mmol·h·bar, produced a low-molecular-weight polymer with a narrow P.D.I. In the case of **1**, it was found that a minimum of 3 200 equiv of 1-hexene were required for successful copolymerization; with a smaller amount of 1-hexene, only polyethylene was isolated. Upon increasing the concentration of 1-hexene above this threshold, both the activity of **1** and the level of monomer incorporation (11.0−13.6%) remained fairly constant; the molecular weight of the polymer, however, was shown to decrease (runs 1−11). Above 8 000 equiv of 1-hexene, no material is recovered, most probably due to catalyst poisoning.

An increase in temperature from 25 to 45 °C led to an order of magnitude decrease in the activity of the system and the molecular weight of the resulting polymer, for example runs 18 and 19. The 1-hexene incorporation fell by 3% (to ca. 10%); however, the P.D.I. of the resulting polymer remained constant. Analysis of the copolymer was carried out by ^{13}C NMR in $CDCl_3$ at room temperature, with the assignment of the microstructure following previous work reported by Hsieh and Randall[64] (Figure 8).

The polymer produced appears to be long chains of polyethylene with isolated units of hexene. The lack of any peaks at ∼40 ppm (indicating the absence of polyhexane blocks within the polymer) and at ∼24 ppm (indicative of alternating sequences of monomers) supports the idea of single incorporation of a 1-hexene monomer into a predominantly polyethylene polymer, which can be explained due to steric crowding around the metal center. ^1H NMR analysis indicated an incorporation of ca. 1 unit of 1-hexene for every 10 units of ethylene polymerized.

4. Conclusions

A new family of highly active vanadium procatalysts bearing a ligand featuring sulfur, nitrogen, and oxygen donor ligands has been synthesized and screened for the homopolymerization of ethylene and copolymerization of ethylene/1-hexene. Catalytic studies suggest that a single active species is responsible for the polymerization and that this species has a certain degree of thermal stability. The nature of the cocatalyst is crucial, with aluminum species containing both alkyl and chloro substituents producing the highest activities; the exclusion of ETA in the reactions leads to a negligible change in activities but does result in a noticeable broadening of the P.D.I.'s of the resulting polymer products. However, any structure−activity relationship discussions are best restricted to the procatalyst because the exact nature of the active species in these vanadium-based systems still remains a mystery. Reduction of the imine function in the procatalyst resulted in poorer activities, a trend that has been noted elsewhere in other systems.[65] When compared with the known FI catalysts reported by Fujita et al.,[46] the inclusion of the additional sulfur atom resulted in higher activities for the vanadium(III) species and comparable activites for the vanadium(IV) species. Furthermore, the polymer produced was found to have a higher molecular weight, particularly at elevated temperatures; in the case of vanadium(IV), a much-narrower P.D.I. was suggestive of a more-controlled polymerization process. Increasing the alkane chain length in the ligand backbone did not result in any noticeable beneficial effects for ethylene homopolymerization.

For the copolymerization of ethylene/1-hexene, the resulting polymer properties and levels of incorporation are again suggestive of a common active species, which in this case is independent of the ligands employed.

Acknowledgment. The University of East Anglia and the EPSRC are thanked for financial support. We thank the EPSRC Mass Spectrometry Service Centre (Swansea, U.K.). We would also like to thank Rapra Scientific Ltd. for GPC measurements and Dr. Myles Cheesman (UEA) for help with recording EPR spectra.

Supporting Information Available: Structures of H_2L^1, H_2L^4, **1**, **3**, and **7** in CIF format. This material is available free of charge via the Internet at http://pubs.acs.org.

IC701461B

(61) Ma, Y. L.; Reardon, D.; Gambarotta, S.; Yap, G. *Organometallics* **1999**, *18*, 2773.
(62) Gambarotta, S.; Reardon, D.; Guan, J.; Yap, G. P. A.; Wilson, D. R. *Organometallics* **2002**, *21*, 4390.
(63) Bialek, M.; Czaja, K. *Polymer* **2000**, *41*, 7899.
(64) Hsieh, E. T.; Randall, J. C. *Macromolecules* **1982**, *15*, 1402.
(65) Britovsek, G. J. P.; Gibson, V. C.; Mastroianni, S.; Oakes, D. C. H.; Redshaw, C.; Solan, G. A.; White, A. J. P.; Williams, D. J. *Eur. J. Inorg. Chem.* **2001**, 431.